Catal Lett (2008) 120:143–147
DOI 10.1007/s10562-007-9266-7

Promoting Effect of CeO_2 on NO_x Reduction with Propene over SnO_2/Al_2O_3 Catalyst Studied with In situ FT-IR Spectroscopy

Zhiming Liu · Kwang Seok Oh · Seong Ihl Woo

Received: 15 June 2007 / Accepted: 26 August 2007 / Published online: 15 September 2007

Abstract The mechanistic cause of the promoting effect of CeO_2 on the activity of SnO_2/Al_2O_3 catalyst for the SCR of NO_x by propene was investigated using X-ray photoelectron spectra (XPS) and in situ Fourier transform infrared (FT-IR) spectroscopy. FT-IR measurements have revealed that the role of CeO_2 on the CeO_2–SnO_2/Al_2O_3 catalyst is to contribute to the formation of formate, acetate and nitrate species, and to promote the reaction between nitrates and hydrocarbon-derived species to form isocyanate (–NCO), which is a reaction intermediate for NO_x reduction.

Keywords CeO_2 · Selective catalytic reduction · NO_x · CeO_2–SnO_2/Al_2O_3 catalyst · XPS · In situ FT-IR

1 Introduction

The selective catalytic reduction of NO_x by hydrocarbons (HC-SCR) under oxygen-rich atmospheres is a potential method to remove NO_x from lean-burn and diesel exhaust [1–12]. SnO_2/Al_2O_3 catalyst is a promising candidate for a NO_x reduction catalyst due to its high stability and activity even in the presence of water and SO_2 [13, 14]. However, the effective temperature is relatively high compared with the temperature of diesel exhaust. Hence, the enhancement of the low-temperature activity of the SnO_2/Al_2O_3 catalyst is desirable.

Our recent research has shown that the addition of 0.5% CeO_2 to a 5% SnO_2/Al_2O_3 catalyst significantly improved its NO_x reduction activity, especially at low temperatures [15]. However, the mechanistic cause of the promoting effect of CeO_2 is still unclear. We have investigated the HC-SCR mechanism over SnO_2/Al_2O_3 catalyst using in situ FT-IR spectroscopy and proposed that hydrocarbon-derived species (formate and acetate) and nitrate species are crucial ad-species in the HC-SCR [16]. It is expected that the addition of CeO_2 will affect the formation and consumption rate of these surface species, and hence the HC-SCR activity of SnO_2/Al_2O_3 catalyst. In this study, we have made in situ FT-IR spectroscopy observations of surface species formed on 0.5% CeO_2–5% SnO_2/Al_2O_3 and 5% SnO_2/Al_2O_3 catalysts to investigate the mechanistic effect of CeO_2 addition during the SCR of NO_x.

2 Experimental

SnO_2/Al_2O_3 and CeO_2–SnO_2/Al_2O_3 catalysts were prepared by a single step sol–gel method. Aluminium boehmite sol was first prepared by hydrolysis of aluminium(III) iso-propoxide (AIP) in hot water (85 °C) with a proper amount of nitric acid, and then mixed with a solution of $SnCl_4$ (or $SnCl_4$ and $Ce(NO_3)_3$). After one day of stirring, the solvents were eliminated by heating under reduced pressure to form a gel. The obtained gel was dried at 120 °C for 24 h, followed by calcination at 600 °C for 4 h in air. The loadings of Sn and Ce were fixed at 5% and 0.5%, respectively.

XPS measurements were conducted on a surface system (LHS-10, SPECS GmbH) equipped with a multi-plate channel detector using Mg Kα radiation. Binding energy was referenced to C 1s at 284.5 eV.

In situ FT-IR spectra were acquired using an in situ cell installed in a Nicolet Magna 560 FT-IR spectrometer with

---

Z. Liu · K. S. Oh · S. I. Woo (✉)
Department of Chemical and Biomolecular Engineering,
Center for Ultramicrochemical Process Systems,
Korea Advanced Institute of Science and Technology, 373-1,
Guseong-dong, Yuseong-gu, Daejeon 305-701, Korea
e-mail: siwoo@kaist.ac.kr

a MCT detector. Prior to each experiment, the catalyst was pressed into a self-supported disc and pretreated in 3% O_2/He at 400 °C for 1 h, followed by cooling to the desired temperature before taking a reference spectrum. A gas mixture was then fed into the cell at a flow rate of 25 $cm^3\ min^{-1}$. The concentrations of NO, C_3H_6 and O_2 in the gas mixture were 2,000 ppm, 2,700 ppm and 3%, respectively. All spectra reported here were taken at a resolution of 4 cm^{-1} for 100 scans.

3 Results and Discussion

3.1 X-ray Photoelectron Spectra

The XPS results of Sn $3d_{5/2}$ spectra for SnO_2/Al_2O_3 and CeO_2–SnO_2/Al_2O_3 catalysts are shown in Fig. 1. The binding energy of Sn $3d_{5/2}$ over SnO_2/Al_2O_3 and CeO_2–SnO_2/Al_2O_3 catalysts are 487.2 and 486.9 eV respectively, both of which are ascribed to Sn(IV) [17]. Previous research has shown that Sn^{4+} is active for the reduction of NO_x [18]. For SnO_2/Al_2O_3, the surface concentration of Sn is 2.4%, whereas the concentration decreases to 1.3% over CeO_2–SnO_2/Al_2O_3 catalyst. Recently Serrano-Ruiz et al. [17] has reported that there is strong interaction between Sn and Ce, stabilizing the oxidation state of Sn. The cerium ions could migrate onto SnO_2 particles, which accounts for the lower surface concentration of Sn over CeO_2–SnO_2/Al_2O_3 catalyst. The presence of Ce thus improves the poor ability to activate hydrocarbon of SnO_2 [18] and it can also contribute to the NO oxidation to NO_2 [19], both of which are important process for the NO_x reduction [3]. The promoting effect of CeO_2 has also been observed on Pt/Al_2O_3 catalyst and it is attributed to the existence of bimetallic (Pt–Ce) interaction [20]. For CeO_2–SnO_2/Al_2O_3 catalyst, the strong interaction between SnO_2 and CeO_2 is also associated with the improved activity.

3.2 Influence of CeO_2 on the Formation of Adsorbed Species

The selective catalytic reduction of NO_x with hydrocarbons is known to proceed through the formation and subsequent reactions of several surface species [21–27]. Formation of oxygenated hydrocarbon species over SnO_2/Al_2O_3 and CeO_2–SnO_2/Al_2O_3 catalysts was examined by in situ IR experiment and the results are shown in Fig. 2. The peaks at 1446, 1474, 1646 and 1670 cm^{-1} can be observed at 100 °C. Over both catalysts, the peaks at 1446 and 1670 cm^{-1} can be assigned to ν_s (COO) of acrylate [28] and acrolein [29], respectively. The characteristic peak at 1474 and 1646 cm^{-1} can be assigned to δ_{as} (CH_3) of propionate and ν_s (C=C) of acrylate [30]. With increasing reaction temperature, the intensities of acrolein and acrylate decreased, while those bands at 1376, 1392, 1590 and 1462 cm^{-1} increased. The bands at 1376, 1392 and 1590 cm^{-1} can be assigned to the ν_s (COO^-), δ(CH) and ν_{as} (COO^-) of adsorbed formate species, respectively [28, 31–33]. The band at 1462 cm^{-1} is attributed to the ν_s (COO^-) of adsorbed acetate species [31, 34]. This indicates that the formation of hydrocarbon oxygenates occurs at relatively high temperatures. The adsorption bands around 2900–3000 cm^{-1} are due to the C-H stretching vibration mode of the adsorbed formate species [34]. It is evident that the intensities of formate and acetate peaks over CeO_2–SnO_2/Al_2O_3 catalyst are stronger than those over SnO_2/Al_2O_3 at the same temperatures. This result suggests that the formation of formate and acetate species derived from the partial oxidation of propene is significantly promoted by the addition of CeO_2 to SnO_2/Al_2O_3 catalyst.

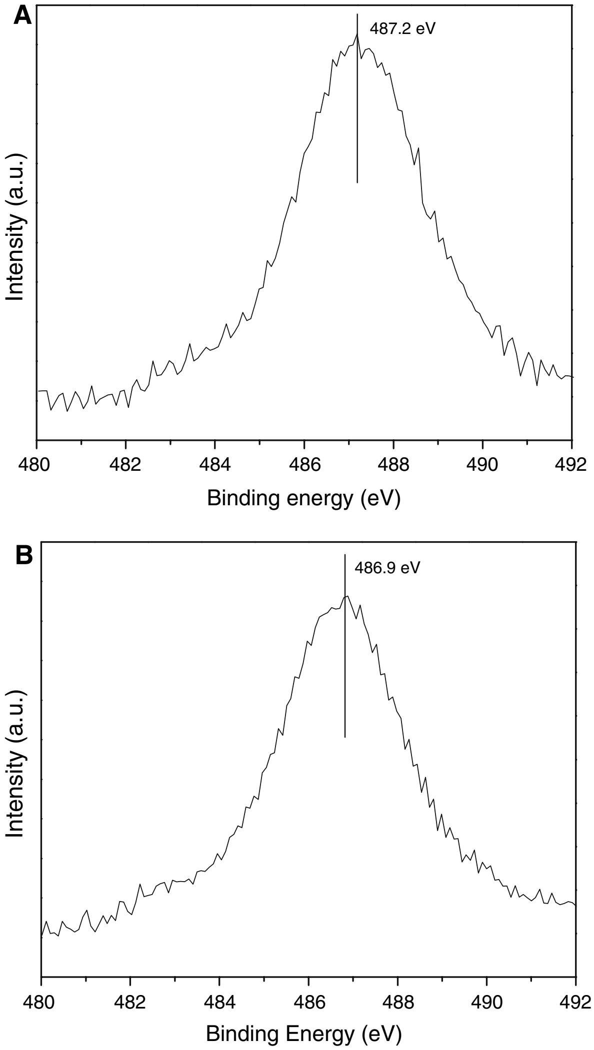

Fig. 1 XPS Sn $3d_{5/2}$ spectra of SnO_2/Al_2O_3 (**A**) and CeO_2–SnO_2/Al_2O_3 (**B**) catalysts

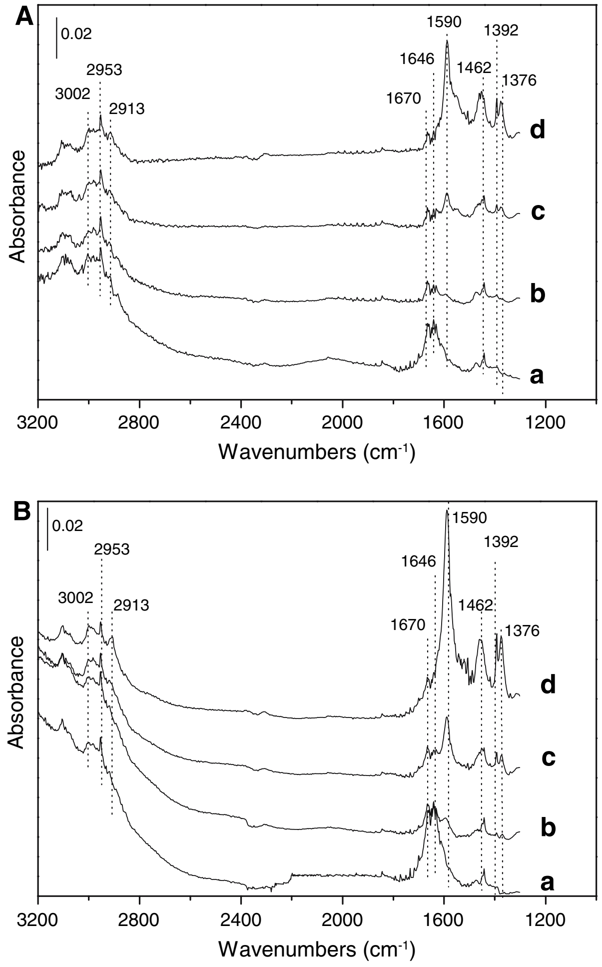

Fig. 2 IR spectra of adsorbed oxygenated hydrocarbon species over SnO_2/Al_2O_3 (**A**) and CeO_2–SnO_2/Al_2O_3 (**B**) at (a) 100 °C, (b) 200 °C, (c) 250 °C, (d) 300 °C. Conditions: C_3H_6 = 2700 ppm, O_2 = 3%

Figure 3 shows the IR spectra of adsorbed nitrate species over SnO_2/Al_2O_3 and CeO_2–SnO_2/Al_2O_3 catalysts at different temperatures in the flowing of NO + O_2. The bands at 1241 and 1552 cm^{-1} can be assigned to the ν_a (ONO) and ν (N=O) of adsorbed monodentate nitrate species [28, 35–37], and the bands at 1303, 1589 and 1621 cm^{-1} to the ν_{as} (ONO) and ν (N=O) of adsorbed bidentate nitrate species and bridging nitrate species, respectively [35–37]. One important phenomenon is that the band intensities of nitrate species increases over CeO_2–SnO_2 /Al_2O_3 catalyst compared with those over SnO_2/Al_2O_3, which indicates that the presence of CeO_2 contributes to the formation of nitrate species.

3.3 Influence of CeO_2 on the Consumption of Adsorbed Species

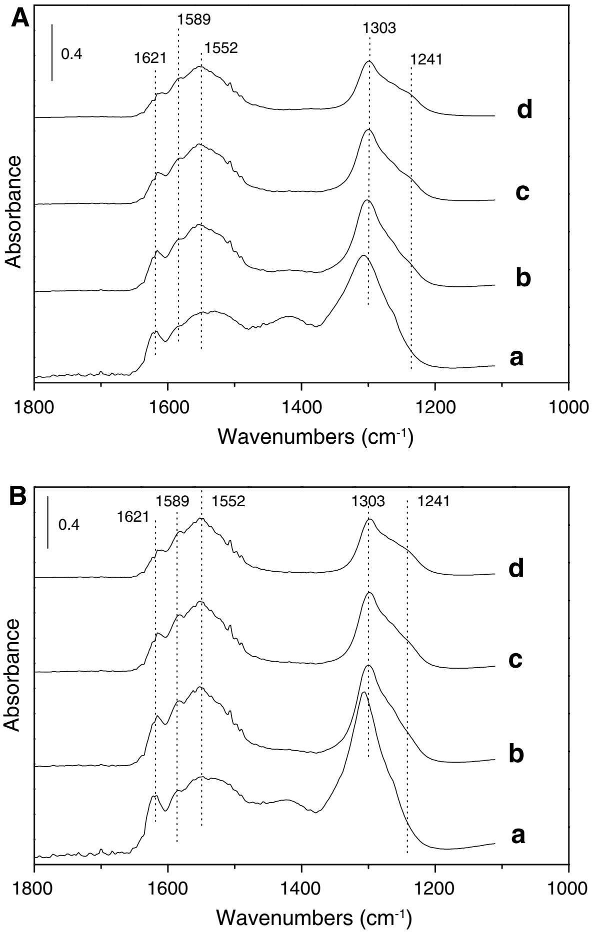

Fig. 3 IR spectra of adsorbed nitrate species over SnO_2/Al_2O_3 (**A**) and CeO_2–SnO_2/Al_2O_3 (**B**) at (a) 100 °C, (b) 200 °C, (c) 250 °C, (d) 300 °C. Conditions: NO = 2000 ppm, O_2 = 3%

The reactivity of adsorbed NO_3^- species towards hydrocarbon-derived species over SnO_2/Al_2O_3 and CeO_2–SnO_2/Al_2O_3 catalysts was evaluated by time-dependent changes of the IR spectra. The catalysts were first exposed to a flow of NO + O_2 for 60 min at 400 °C, and the flowing gas was subsequently switched to He for 30 min to remove gas phase NO_x and any weakly adsorbed NO_x species. The gas was then switched to C_3H_6 + O_2 for 30 min and the IR spectra were recorded (see Fig. 4). Over SnO_2/Al_2O_3 catalyst, the band characteristic of the monodentate nitrate (1249 cm^{-1}) almost completely disappeared while that of bidentate nitrate (1303 cm^{-1}) remains almost unchanged, indicating that monodentate nitrate is reactive species and bidentate nitrate is spectator species. In contrast, after exposing the CeO_2–SnO_2/Al_2O_3 catalyst to C_3H_6 + O_2 for 30 min, besides the almost completely disappearing of the monodentate nitrate, the intensity of bidentate nitrate peak also significantly decreased. This fact indicates that over the CeO_2–SnO_2/Al_2O_3 catalyst, both monodentate and bidentate nitrates are reactive species. Thus, the presence of CeO_2 not only contributes to the formation of nitrates, but also makes bidentate nitrate become active for the NO_x reduction.

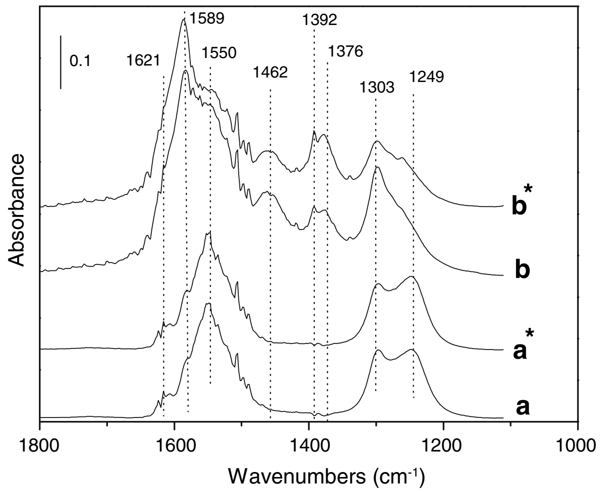

Fig. 4 IR spectra of adsorbed species over SnO_2/Al_2O_3 (a, b) and CeO_2–SnO_2/Al_2O_3 (a^*, b^*) at 400 °C taken after (a, a^*) pre-exposing in a flow of NO + O_2 for 60 min at 400 °C, followed by He purge for 30 min and then change the gas to (b, b^*) C_3H_6 + O_2 for 30 min

The reactivity of adsorbed hydrocarbon oxygenates towards nitrate species over SnO_2/Al_2O_3 and CeO_2–SnO_2/Al_2O_3 catalysts was also evaluated by time-dependent changes of the IR spectra. The catalysts were first exposed to a flow of C_3H_6 + O_2 for 60 min at 400 °C, subsequently the flowing gas was switched to He for 30 min. The catalysts were then exposed to a flow of NO + O_2 for 30 min and the IR spectra were recorded (see Fig. 5). Over the two catalysts, both the formate (1376, 1392 and 1590 cm^{-1}) and acetate (1462 cm^{-1}) bands decreased on exposure to NO + O_2 for 30 min, while the band intensities due to monodentate nitrate (1249 cm^{-1} and 1550 cm^{-1}) and bidentate nitrate (1303 cm^{-1}) increased. It should be noted that over the CeO_2–SnO_2/Al_2O_3 catalyst, the acetate band almost disappeared after exposing to NO + O_2 for 30 min, indicating that the presence of CeO_2 promotes the reaction rate between the acetate and nitrate species, which is an important step in the HC-SCR over SnO_2/Al_2O_3 catalyst [16]. It also indicates that over the CeO_2–SnO_2/Al_2O_3 catalyst, acetate is more reactive than formate.

Since it has been reported that –NCO species is a reaction intermediate for NO reduction with hydrocarbons [28, 33, 35], Figure 6 shows the dynamic changes of the adsorption peak area of –NCO species (2225–2260 cm^{-1}) over SnO_2/Al_2O_3 and CeO_2–SnO_2/Al_2O_3 catalysts as a function of time in a flow of NO + O_2 at 400 °C. Over both catalysts, the absorption peak area of –NCO rapidly increases and then gradually decreases with time on stream after the gas change. This suggests that the –NCO species is formed by the reaction of NO_3^- and hydrocarbon-derived species. It is evident that the peak area is larger and the rate of formation higher for CeO_2–SnO_2/Al_2O_3 than for SnO_2/Al_2O_3, corresponding to their NO_x reduction activities [15].

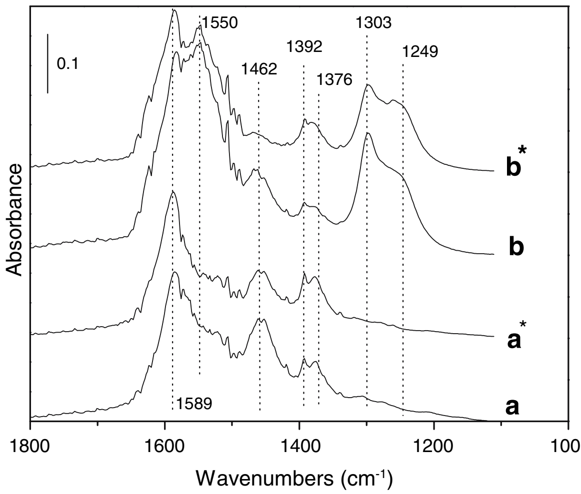

Fig. 5 IR spectra of adsorbed species over SnO_2/Al_2O_3 (a, b) and CeO_2–SnO_2/Al_2O_3 (a^*, b^*) at 400 °C taken after (a, a^*) pre-exposing in a flow of C_3H_6 + O_2 for 60 min at 400 °C, followed by He purge for 30 min and then change the gas to (b, b^*) NO + O_2 for 30 min

Based on the FT-IR studies, we have proposed a simplified reaction scheme for the NO_x reduction with propene over SnO_2/Al_2O_3 catalyst [16]. Therein, the reaction starts with the formation of both adsorbed nitrates via NO oxidation by O_2, and formate and acetate species via the partial oxidation of propene. The reaction between the two kinds of adsorbed species then leads to the formation of nitrogen-containing organic species, such as –NCO species, which then react with NO_x to form N_2. Our present study shows that the presence of CeO_2 over CeO_2–SnO_2/Al_2O_3 catalyst not only contributes to the formation of

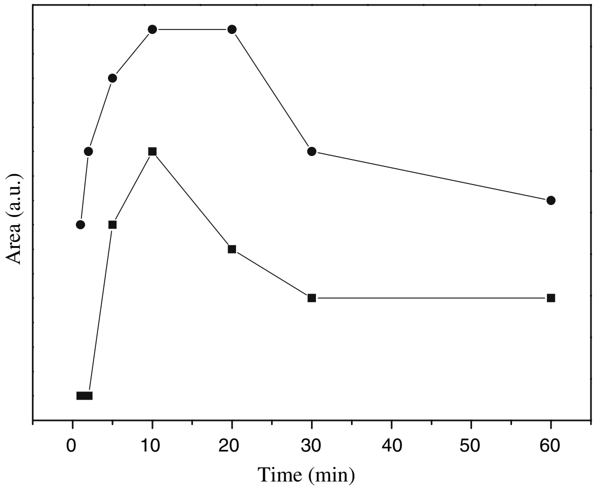

Fig. 6 Dynamic changes of the integrated area of –NCO species (2225–2260cm^{-1}) over SnO_2/Al_2O_3 (■) and CeO_2-SnO_2/Al_2O_3 (•) as a function of time in a flow of NO + O_2 at 400 °C. Before the measurement, the two catalysts were pre-exposed in a flow of C_3H_6 + O_2 for 60 min at 400 °C, followed by He purge for 30 min and then change the gas to NO + O_2, respectively

oxygenated hydrocarbon species (formate and acetate) and nitrate species, which are important intermediates for NO_x reduction, but also improves the reactivity of the nitrate species. As a result, more –NCO intermediates are formed and the following steps leading to N_2 formation become faster over CeO_2–SnO_2/Al_2O_3 catalyst.

4 Conclusions

The promoting effect of CeO_2 on the activity of SnO_2/Al_2O_3 catalyst during the SCR of NO_x has been discussed on the basis of XPS analysis and FT-IR measurements of surface species formation and consumption over SnO_2/Al_2O_3 and CeO_2–SnO_2/Al_2O_3 catalysts. It is proposed that there is strong interaction between CeO_2–SnO_2, which keeps Sn active. The role of CeO_2 is to contribute to the formation of hydrocarbon-derived species (formate and acetate) and nitrate species, which results in a higher surface concentration of –NCO species, and increased efficiency of NO_x reduction over the CeO_2–SnO_2/Al_2O_3 catalyst.

Acknowledgements This research was funded by the Center for Ultramicrochemical Process Systems (CUPS) supported by KOSEF (2005) and Z. Liu was supported by BK21 postdoctoral fellowship.

References

1. Shelef M (1995) Chem Rev 95:209
2. Burch R, Breen JP, Meunier FC (2002) Appl Catal B 39:283
3. Liu ZM, Woo SI (2006) Catal Rev Sci Eng 48:43
4. Iwamoto M, Yahiro H, Shundo S, Yu-u Y, Mizuno N (1991) Appl Catal 15:69
5. Aylor AW, Lobree LJ, Reimer JA, Bell AT (1997) J Catal 170:390
6. Cant NW, Liu IOY (2000) Catal Today 63:133
7. Liu ZM, Woo SI Catal. Surv. Asia (in press)
8. Xin M, Hwang IC, Kim DH, Cho SI, Woo SI (1999) Appl Catal B 21:183
9. Decyk P, Kim DK, Woo SI (2001) J Catal 203:369
10. Jeon JY, Kim HY, Woo SI (2002) Chem Lett 2:246
11. Woo SI, Kim DK, Park YK, Kim MR, Decyk P (2003) Catal Lett 85:69
12. Jeon JY, Kim HY, Woo SI (2003) Appl Catal B 44:311
13. Kung MC, Park PW, Kim D-W, Kung HH (1999) J Catal 181:1
14. Li J, Hao J, Fu L, Liu Z, Cui X (2004) Catal Today 90:215
15. Liu ZM, Oh KS, Woo SI (2006) Catal Lett 106:35
16. Liu ZM, Woo SI, Lee WS (2006) J Phys Chem B 110:26019
17. Serrano-Ruiz JC, Huber GW, Sánchez-Castillo MA, Dumesic JA, Rodríguez-Reinoso F, Sepúlveda-Escribano A (2006) J Catal 241:378
18. Park PW, Kung HH, Kim D-W, Kung MC (1999) J Catal 184:440
19. Li Z, Flytzani-Stephanopoulos M (1999) J Catal 182:313
20. Tiernan MJ, Finlayson OE (1998) Appl Catal B 19:23
21. Smits RH, Iwasawa Y (1995) Appl Catal B 6:201
22. Adelman BJ, Beutel T, Lei G-D, Sachtler WMH (1996) Appl Catal B 11:1
23. Martens JA, Cauvel A, Francis A, Hermans C, Joyat F, Remy M, Keung M, Lievens J, Jacobs PA (1998) Angew Chem Int Ed 37:1901
24. Hwang IC, Kim DH, Woo SI (1998) Catal Today 44:47
25. Hwagn IC, Kim DH, Woo SI (1996) Catal Lett 42:177
26. Xin M, Hwang IC, Woo SI (1997) Catal Today 38:187
27. Xin M, Hwang IC, Woo SI (1997) J Phys Chem B 101:9005
28. Meunier FC, Zuzaniuk V, Breen JP, Olsson M, Ross JRH (2000) Catal Today 59:287
29. Hayes NW, Joyner RW, Shpiro ES (1996) Appl Catal B 8:343
30. Shibata J, Shimizu K, Satokawa S, Satsuma A, Hattori T (2003) Phys Chem Chem Phys 5:2154
31. He C, Paulus M, Find J, Nickl JA, Eberle H-J, Spengler J, Chu W, Köhler K (2005) J Phys Chem B 109:15906
32. Sato K, Yoshinari T, Kintaichi Y, Haneda M, Hamada H (2003) Appl Catal B 44:67
33. Haneda M, Bion N, Daturi M, Saussey J, Lavalley J, Duprez D, Hamada H (2002) J Catal 206:114
34. Haneda M, Kintaichi Y, Bion N, Hamada H (2003) Appl Catal B 42:57
35. Shimizu K, Shibata J, Yoshida H, Satsuma A, Hattori T (2001) Appl Catal B 30:151
36. Yu Y, He H, Feng Q, Gao H, Yang X (2004) Appl Catal B 49:159
37. Eränen K, Klingstedt F, Arve K, Lindfors L, Murzin DY (2004) J Catal 227:328